Liquid-Drop Model for Crystalline Metals: Vacancy-Formation, Cohesive, and Face-Dependent Surface Energies

John P. Perdew and Yue Wang
Department of Physics and Quantum Theory Group, Tulane University, New Orleans, Louisiana 70118

Eberhard Engel
Department of Physics, University of Toronto, Toronto, Ontario, Canada M5S 1A7
(Received 16 July 1990)

The energy of a metallic crystal is expressed as a sum of volume, surface, and curvature terms. The fully self-consistent solution of a simplified problem shows that, in the absence of shell-structure effects, this expression can be accurate even for atomic-scale properties. Thus the liquid-drop model, originally developed for finite systems (nuclei), may actually be more appropriate for infinite ones (metals). First applications are made to the face dependence of the surface energy and to monovacancy-formation and cohesive energies. Predictions of the model may be tested by experiment or by fully self-consistent Kohn-Sham calculations.

PACS numbers: 71.45.Nt, 61.70.Bv, 68.35.Md, 71.45.Jp

The total energy of an extended system of volume V and surface area A is

$$E=\alpha V+\sigma A+\tfrac{1}{2}\gamma\int dA\,R^{-1}, \quad (1)$$

where α, σ, and γ are intrinsic volume, surface, and curvature energies (determined largely by the bulk density and nature of the constituent species), and R^{-1} is the local curvature of surface-area element dA. The leading term of Eq. (1) may also be written $\alpha V=\varepsilon N$, where N is the number of constituent particles and ε is the energy per particle in the limit $V/A\rightarrow\infty$. The physics of Eq. (1) is explained in a recent monograph[1] on classical fluids: In a system with $\sigma>0$ and $\gamma>0$, the energy minimizes when each particle has an environment that is as bulklike as possible, i.e., when the surface is as small in area and as concave as it can be for a given volume. This liquid-drop model (sometimes neglecting the curvature energy) has long been useful in nuclear physics,[2] despite errors arising from the shell structure of finite systems. We propose to use Eq. (1) in solid-state physics, for the description of inhomogeneous neutral metals.

Some of the properties we shall discuss, such as the formation energy of a monovacancy or the crystal-face dependence of the metallic surface energy, arise in the limit $V/A\rightarrow\infty$, in which the one-electron levels tend to a continuum and shell-structure effects disappear. These effects are also absent for *finite* V/A within a continuum approximation such as the fourth-order density-gradient expansion[3] for the kinetic energy or the local-density representation for exchange and correlation,[4] which together constitute the Thomas-Fermi-Dirac-Gombas-Weizsäcker-4 (TFDGW4) approximation. In fact, our present study was motivated by the results of our recent solution[5] of the TFDGW4 Euler equation for jellium spheres (Table I), following the method of Ref. 6. We now describe those results.

In the jellium model[7] of a metallic cluster, the positive charge on the ions is smeared into a background of uniform density $\bar{n}=3/4\pi r_s^3$ inside a spherical Gibbs surface of radius $R=N^{1/3}r_s$, where N is the number of electrons needed to neutralize the background. Taking the correlation energy from Ref. 8, we find σ and γ from fits to calculated total energies for spheres of *large* N (up to 10^6 in Ref. 5). To our knowledge, Ref. 5 is the first fully self-consistent study of size dependence in the asymptotic limit $V/A\rightarrow\infty$. A surprising result of this study is displayed in Table I: Equation (1) predicts the energy per electron E/N accurately (within 0.03 eV) *even for* $N=1$, for which

$$E\approx\varepsilon+\sigma 4\pi r_s^2+\gamma 2\pi r_s \quad (2)$$

is the negative of the energy needed to remove the electron and disperse the background ($E=-I+3e^2/5r_s$, where I is the ionization energy). From Table I, we tentatively conclude that the total energy of a neutral metal (in the absence of shell structure) is accurately represented by Eq. (1), even for surfaces that vary on the *atomic* scale.

In a first application of this elementary perspective, we

TABLE I. Within a continuum approximation for the density functional $E[n]$, the total energy E of a neutral one-electron ($N=1$) jellium sphere is accurately represented by the asymptotic ($N\rightarrow\infty$) form of Eq. (1) (from the TFDGW4 calculation of Ref. 5).

r_s (bohrs)	ε (eV)	$\varepsilon+\sigma 4\pi r_s^2$ (eV)	$\varepsilon+\sigma 4\pi r_s^2+\gamma 2\pi r_s$	E (eV)
2	0.065	−0.767	−0.206	−0.172
4	−2.103	−1.623	−1.445	−1.459
6	−1.933	−1.548	−1.478	−1.478

shall calculate the crystal-face dependence of the metallic surface energy. A "planar" crystal surface, formed by cutting along the boundaries of the Wigner-Seitz unit cells and smoothing the resultant sharp corners, is actually corrugated on the atomic scale.[9] Thus the microscopic area A of Eq. (1) is greater than the macroscopic or Gibbs-plane area $\bar{A}$ by a "corrugation factor" $A/\bar{A} > 1$. Moreover, the curvature term of Eq. (1) vanishes, since every microscopic "hill" is paired to a microscopic "valley" with equal and opposite energy of curvature. Thus, we propose that the face-dependent surface energy is

$$\sigma_{\text{face}} = \sigma A/\bar{A}\,, \tag{3}$$

where σ is the intrinsic or flat-surface energy.

Evaluation of the corrugation factor could be a tedious geometric problem for each crystal structure and face. But, for monatomic nearly-close-packed crystals (face-centered cubic or fcc, body-centered cubic or bcc, hexagonal close packed or hcp with near-ideal $c/a \approx 1.633$), the Wigner-Seitz polyhedral unit cell may be replaced by a Wigner-Seitz spherical cell of radius $r_0 = z^{1/3} r_s$, where z is the valence. Let d be the distance between neighboring lattice planes parallel to the surface. Then each Wigner-Seitz spherical cell in the first lattice plane is intersected by the planar Gibbs surface, as shown in Fig. 1. If no sphere from the second lattice plane is so intersected [i.e., if $3d/2 > r_0$, as is the case for all faces considered here except bcc (111)], then the corrugation factor is simply the ratio of the area $2\pi r_0(r_0 - d/2)$ of that part of the spherical-cell surface lying outside the Gibbs plane to the area $\pi[r_0^2 - (d/2)^2]$ of that part's projection onto this plane:

$$A/\bar{A} = 2/(1 + d/2r_0)\,. \tag{4}$$

This factor is presented in Table II for some common crystal faces, using values of d/r_0 from Table IV of Ref. 10. Note that the number of atoms per unit area of Gibbs surface in the first lattice plane is $3d/4\pi r_0^3$, so the surface energy predicted by Eqs. (3) and (4) is higher for a less densely packed face, as expected.[11-13]

As shown in Table III, this conceptually simple, nonempirical, *geometric* theory for the face dependence of the metallic surface energy produces results that fall within the range of those predicted by detailed microscopic calculations or semiempirical models. Specifically, we compare our surface-energy anisotropies with those predicted by the second-order pseudopotential perturbation theory of Rose and Dobson,[11] the variational Kohn-Sham density-matrix calculation of Bohnen and Ying,[12] and the equivalent-crystal model of Smith and Banerjea.[13] Fully self-consistent Kohn-Sham[4] calculations, or experiments, are needed to determine which

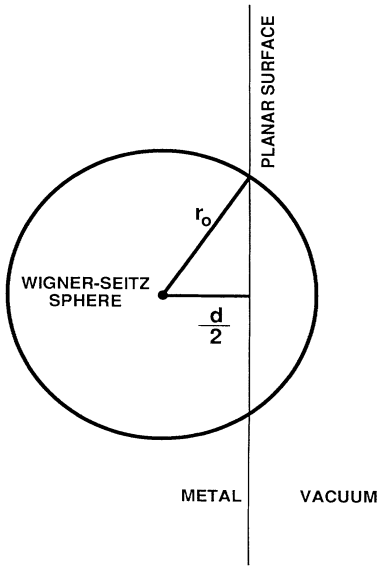

FIG. 1. A Wigner-Seitz spherical cell in the first lattice plane, intersected by the planar Gibbs surface of the metal.

TABLE II. Atomic corrugation factors $A/\bar{A}$ or Eq. (4) for common crystal faces.

Crystal	$A/\bar{A}$
fcc (111)	1.150
(100)	1.220
(110)	1.377
bcc (110)	1.164
(100)	1.327
(111)	1.547[a]
hcp (0001)	1.150

[a]Inclusion of the contribution from the second lattice plane changes the bcc (111) value to 1.451.

TABLE III. Theoretical surface-energy anisotropies. RD: Rose and Dobson (Ref. 11). SB: Smith and Banerjea (Ref. 13). BY: Bohnen and Ying (Ref. 12). LDM: liquid-drop model [Eqs. (3) and (4)]. (RD and BY are partially self-consistent Kohn-Sham pseudopotential calculations; SB is a semiempirical model for the anisotropy.)

		RD	SB	LDM
fcc metals:				
Al	$\sigma_{100}/\sigma_{111}$	1.09	1.39	1.06
	$\sigma_{110}/\sigma_{111}$	1.6	1.42	1.20
Cu	$\sigma_{100}/\sigma_{111}$	···	1.30	1.06
	$\sigma_{110}/\sigma_{111}$	···	1.24	1.20
		RD	BY	LDM
bcc metals:				
Na	$\sigma_{100}/\sigma_{110}$	1.14	1.18	1.14
K	$\sigma_{100}/\sigma_{110}$	1.14	1.18	1.14
Rb	$\sigma_{100}/\sigma_{110}$	1.14	1.23	1.14
Cs	$\sigma_{100}/\sigma_{110}$	1.33	1.22	1.14

theory works best. (In the case of Cu, the self-consistent calculations listed in Ref. 13 yield $\sigma_{100}/\sigma_{111}=1.095$, in reasonable agreement with the result of our liquid-drop model, but no firm conclusion can be drawn since the two self-consistent calculations were done differently.)

Experiment[14,15] suggests that surface energies vary by no more than 10%–20% among various faces of the cubic metals. The predictions of the liquid-drop model (Tables II and III) stand in reasonable agreement with this observation, while the surface energies calculated for bcc Fe and W by the equivalent-crystal model (Table I of Ref. 13) display variations closer to 100%.

We turn now to the curvature energy γ. The shell-structure effects present in finite metallic clusters make it difficult to extract accurate values of γ either from Kohn-Sham orbital calculations[16] or from experiment. But shell effects are absent for a *vacancy* in an infinite metal, which we propose as an ideal system for extraction of γ. In particular, the monovacancy-formation energy[17–19] $\varepsilon_{\rm vac}$ is the energy required to move an atom from the interior of the metal to the surface, leaving behind a "hole" of radius r_0 and *negative* curvature $-1/r_0$. Motivated again by Table I, we apply Eq. (1) to find

$$\varepsilon_{\rm vac}\approx\sigma 4\pi r_0^2-\gamma 2\pi r_0 . \tag{5}$$

From Eq. (5), plus measured vacancy-formation energies and surface energies, we determine the curvature energies γ for real metals presented in Table IV. The intrinsic or flat-surface energy σ is constructed from the measured liquid-metal surface tension, extrapolated to zero temperature[20] and divided by an atomic corrugation factor of 1.2. [The liquid-metal surface energy is probably close[11] to that of a low-energy crystal face like fcc (111) or bcc (110).] The curvature energies γ found for real metals in Table IV have the same sign and order of magnitude as those which have been computed for jellium.[5,16]

The cohesive energy[21] is the energy per atom needed to separate the metal into neutral atoms. Neglecting shell-structure effects, this is just the energy needed to create the curved surface of the free atom, which Eq. (1) predicts to be

$$\varepsilon_{\rm coh}\approx\sigma 4\pi r_0^2+\gamma 2\pi r_0 . \tag{6}$$

A cruder approximation, which retains just the first term on the right-hand side of Eq. (6), is well known.[20,22,23] Table IV shows that Eq. (6) gives an accurate account of the cohesive energies of the monovalent metals, using values of σ and γ already determined from the preceding paragraph. [It follows from Eqs. (5) and (6) that $\varepsilon_{\rm vac}+\varepsilon_{\rm coh}\approx\sigma 8\pi r_0^2$ for the monovalents.] However, Eq. (6) is less satisfactory for divalent and polyvalent metals, for which shell effects in the free atom cannot be neglected, and its success for the monovalents is unexplained.

In summary, we have presented a liquid-drop model for a neutral inhomogeneous metal. There are three intrinsic parameters (ε, σ, and γ), which may be measured

TABLE IV. The intrinsic surface energy σ and curvature energy γ of a monovalent ($z=1$) metal determine the monovacancy-formation energy $\varepsilon_{\rm vac}$ and cohesive energy $\varepsilon_{\rm coh}$, via Eqs. (5) and (6). Here r_0, σ, $\varepsilon_{\rm vac}$, and $\varepsilon_{\rm coh}$ are experimental values; γ is constructed from Eq. (5). (The extra stability of the divalent atoms due to subshell closure makes their cohesive energies smaller than the predictions of the liquid-drop model.)

z	Metal	r_0 (bohrs)	$\varepsilon_{\rm vac}$ (eV)	$\sigma 4\pi r_0^2$ [d] (eV)	γ (eV/bohr)	$\sigma 4\pi r_0^2+\gamma 2\pi r_0$	$\varepsilon_{\rm coh}$ [e] (eV)
1	Cu	2.67	1.28 [a]	2.34	0.063	3.40	3.49
	Ag	3.02	1.11 [a]	2.08	0.051	3.05	2.95
	Au	3.01	0.89 [a]	2.50	0.085	4.11	3.81
	Li	3.25	0.34 [b]	1.01	0.0328	1.68	1.63
	Na	3.93	0.42 [b]	0.74	0.0130	1.06	1.11
	K	4.86	0.39 [b]	0.63	0.0079	0.87	0.93
	Rb	5.20	0.27 [c]	0.58	0.0095	0.89	0.85
	Cs	5.62	0.28 [b]	0.55	0.0076	0.82	0.80
2	Mg	3.35	0.9 [a]	1.61	0.034	2.32	1.51
	Zn	2.90	0.54 [a]	1.53	0.054	2.52	1.35
	Cd	3.26	0.52 [a]	1.48	0.047	2.44	1.16
3	Al	2.99	0.66 [a]	1.86	0.064	3.06	3.39
	In	3.48	0.55 [a]	1.55	0.046	2.55	2.52
	Tl	3.58	0.46 [a]	1.41	0.042	2.36	1.88
4	Sn	3.52	0.54 [a]	1.61	0.048	2.68	3.14
	Pb	3.65	0.5 [a]	1.45	0.041	2.40	2.03

[a]Reference 18.
[b]Reference 17.
[c]Reference 19.
[d]Reference 20.
[e]Reference 21.

or calculated from first principles. (Intrinsic surface energies σ are calculated in Ref. 24, without appeal to a corrugation factor.) This model provides a simple and seemingly accurate account of face-dependent surface energies, monovacancy-formation energies, and (for monovalents) cohesive energies. Applications to other atomic-scale inhomogeneities might also prove interesting. [Note that the model cannot explain the different reconstruction properties of (110) surfaces of Cu, Ag, and Au.]

Based upon the results of Table I, our confidence in the liquid-drop model is highest for simple metals of infinite volume, and declines as we pass to noble metals, transition metals, and finite systems (e.g., single atoms). Thus we believe that the model can predict the energies and equilibrium shapes of voids more reliably than those of metallic clusters, where shell-structure effects may be important. Further tests are needed, beyond those presented here.

Because of the uncertainties of measured surface and vacancy-formation energies, the most precise tests are likely to be comparisons with the results of fully self-consistent Kohn-Sham[4] calculations: (1) Surface energies could be calculated accurately for different faces of various close-packed metals, and their ratios compared with the predictions of Eqs. (3) and (4). (2) The surface and curvature energies of jellium (or stabilized pseudo-jellium[24]) could be found from the calculated energies of large spherical voids, and used to test Eq. (5) against computed monovacancy-formation energies. (Analysis of Fig. 5 of Ref. 25 suggests that the liquid-drop model might pass this test for jellium, with $\gamma \approx 0.037$ eV/bohr at $r_s = 2.07$ bohrs and $\gamma \approx 0.012$ eV/bohr at $r_s = 3.93$ bohrs.)

This work was supported by the National Science Foundation under Grant No. DMR 88-17866 (J.P.P. and Y.W.), and by a NATO Postdoctoral Fellowship (E.E.). One of us (J.P.P.) acknowledges discussions of nuclear physics with A. L. Goodman and G. T. Rosensteel, and helpful private communications from R. M. Nieminen and P. H. Dederichs. One of us (E.E.) thanks S. H. Vosko for encouragement and support through the Natural Sciences and Engineering Research Council of Canada and the Ontario Centre for Large Scale Computation.

[1]J. S. Rowlinson and B. Widom, *Molecular Theory of Capillarity* (Clarendon, Oxford, 1982).

[2]R. W. Hasse and W. D. Myers, *Geometrical Relationships of Macroscopic Nuclear Physics* (Springer-Verlag, Berlin, 1988).

[3]C. H. Hodges, Can. J. Phys. **51**, 1428 (1973).

[4]P. Hohenberg and W. Kohn, Phys. Rev. **136**, B864 (1964); W. Kohn and L. J. Sham, Phys. Rev. **140**, A1133 (1965).

[5]E. Engel and J. P. Perdew, Phys. Rev. B **43**, 1331 (1991).

[6]E. Engel and R. M. Dreizler, J. Phys. B **22**, 1901 (1989).

[7]M. Manninen, Phys. Rev. B **34**, 6886 (1986).

[8]S. H. Vosko, L. Wilk, and M. Nusair, Can. J. Phys. **58**, 1200 (1980).

[9]R. Smoluchowski, Phys. Rev. **60**, 661 (1941).

[10]R. Monnier and J. P. Perdew, Phys. Rev. B **17**, 2595 (1978); **22**, 1124 (E) (1980).

[11]J. H. Rose and J. F. Dobson, Solid State Commun. **37**, 91 (1981).

[12]K.-P. Bohnen and S. C. Ying, Solid State Commun. **30**, 301 (1979).

[13]J. R. Smith and A. Banerjea, Phys. Rev. Lett. **59**, 2451 (1987).

[14]For a compilation of experimental papers, see footnote 155 of N. D. Lang, Solid State Phys. **28**, 225 (1973).

[15]W. R. Tyson, R. A. Ayres, and D. F. Stein, Acta. Metall. **21**, 621 (1973).

[16]C. A. Utreras-Díaz and H. B. Shore, Phys. Rev. B **40**, 10345 (1989).

[17]M. Manninen, R. Nieminen, P. Hautojärvi, and J. Arponen, Phys. Rev. B **12**, 4012 (1975).

[18]H.-E. Schaefer, Phys. Status Solidi A **102**, 47 (1987).

[19]Ya. A. Kraftmacher and P. G. Strelkov, in *Vacancies and Interstitials in Metals,* edited by A. Seeger, D. Schumacher, W. Schilling, and J. Diehl (North-Holland, Amsterdam, 1970), p. 59.

[20]W. R. Tyson and W. A. Miller, Surf. Sci. **62**, 267 (1977).

[21]C. Kittel, *Introduction to Solid State Physics* (Wiley, New York, 1986), 6th ed.

[22]J. H. Rose, J. P. Vary, and J. R. Smith, Phys. Rev. Lett. **53**, 344 (1984). This paper predicts universal scaling relations which our jellium results do not obey, except roughly at $r_s \approx 4$ (where bulk jellium is stable.) Define the cohesive energy $\varepsilon_{\rm coh}$ as the difference between E (for $N=1$) and ε. Then we find, from Table I, $\sigma 4\pi r_s^2/\varepsilon_{\rm coh} = 3.52$, 0.75, and 0.84 for $r_s = 2$, 4, and 6, respectively, while scaling predicts 0.82. Similarly we find $\gamma 2\pi r_s/\varepsilon_{\rm coh} = -2.37$, 0.28, and 0.15, while scaling predicts 0.7. For the real monovalents of Table IV, $\sigma 4\pi r_s^2/\varepsilon_{\rm coh} = 0.67 \pm 0.05$ and $\gamma 2\pi r_s/\varepsilon_{\rm coh} = 0.34 \pm 0.07$.

[23]J. P. Perdew, Phys. Rev. B **37**, 6175 (1988).

[24]J. P. Perdew, H. Q. Tran, and E. D. Smith, Phys. Rev. B **42**, 11627 (1990).

[25]M. Manninen and R. M. Nieminen, J. Phys. F **8**, 2243 (1978).